JACC: CARDIOVASCULAR IMAGING
VOL. 9, NO. 1, 2016

ISSN 1936-878X/$36.00
PUBLISHED BY ELSEVIER
http://dx.doi.org/10.1016/j.jcmg.2015.11.002

T1 Mapping by CMR Imaging

From Histological Validation to Clinical Implication

Andreas A. Kammerlander, MD,* Beatrice A. Marzluf, MD, MSc,* Caroline Zotter-Tufaro, MSc,* Stefan Aschauer, MD,* Franz Duca, MD,* Alina Bachmann, MD,* Klaus Knechtelsdorfer,* Matthias Wiesinger,* Stefan Pfaffenberger, MD,* Andreas Greiser, PhD,† Irene M. Lang, MD,* Diana Bonderman, MD,* Julia Mascherbauer, MD*

ABSTRACT

OBJECTIVES The purpose of this study was to prospectively investigate the diagnostic and prognostic impact of cardiac magnetic resonance (CMR) T1 mapping and validate it against left ventricular biopsies.

BACKGROUND Extracellular volume (ECV) expansion is a key feature of heart failure. CMR T1 mapping has been developed as a noninvasive technique to estimate ECV; however, the diagnostic and prognostic impacts of this technique have not been well established.

METHODS A total of 473 consecutive patients referred for CMR (49.5% female, age 57.8 ± 17.1 years) without hypertrophic cardiomyopathy, cardiac amyloidosis, or Anderson-Fabry disease were studied. T1 mapping with the modified Look-Locker inversion recovery (MOLLI) sequence was used for ECV calculation (CMR-ECV). For methodological validation, 36 patients also underwent left ventricular biopsy, and ECV was quantified by TissueFAXS analysis (TissueFAXS-ECV). To assess the prognostic value of CMR-ECV, its association with hospitalization for cardiovascular reasons or cardiac death was tested in a multivariable Cox regression model.

RESULTS TissueFAXS-ECV was 26.3 ± 7.2% and was significantly correlated with CMR-ECV ($r = 0.493$, $p = 0.002$). Patients were followed up for 13.3 ± 9.0 months and divided into CMR-ECV tertiles for Kaplan-Meier analysis (tertiles were ≤25.7%, 25.8% to 28.5%, and ≥28.6%). Significantly higher event rates were observed in patients with higher CMR-ECV (log-rank $p = 0.013$). By multivariable Cox regression analysis, CMR-ECV was independently associated with outcome among imaging variables ($p = 0.004$) but not after adjustment for clinical parameters.

CONCLUSIONS CMR T1 mapping allows accurate noninvasive quantification of ECV and is independently associated with event-free survival among imaging parameters. Its prognostic value on top of established clinical risk factors warrants further investigation in long-term studies. (J Am Coll Cardiol Img 2016;9:14–23) © 2016 by the American College of Cardiology Foundation.

Extracellular matrix expansion is a hallmark of heart failure. Data from animal and human studies suggest that increased extracellular volume (ECV) is a key finding in both systolic and diastolic heart failure regardless of the cause of the cardiomyopathy (1–7). Given the important prognostic role of myocardial extracellular matrix expansion, a simple and safe method for its quantification is most desirable. Recently, the ability of cardiac magnetic resonance (CMR) to quantify myocardial tissue characteristics by measuring the longitudinal relaxation (T1) time has been demonstrated (8–15). Several

From the *Division of Cardiology, Medical University of Vienna, Vienna, Austria; and †Siemens Healthcare GmbH, Erlangen, Germany. This study received support from the Austrian Society of Cardiology (Dr. Mascherbauer), the Österreichischer Herzfonds (Dr. Mascherbauer) and the Austrian fellowship grant KLI 245 (to Dr. Mascherbauer) and KLI 246 (Dr. Bonderman). Siemens Healthcare GmbH (Erlangen, Germany) provided the T1-mapping prototype as a work-in-progress package but had no influence on study design, data processing, or statistical analysis. Dr. Greiser is an employee of Siemens Healthcare GmbH. Dr. Lang has received grants and speakers' fees from Actelion Pharmaceuticals, Bayer, United Therapeutics, and AOP Orphan Pharmaceuticals. All other authors have reported that they have no relationships relevant to the contents of this paper to disclose.

Manuscript received August 19, 2015; revised manuscript received October 30, 2015, accepted November 3, 2015.

approaches have been studied (16); however, native T1 mapping and the calculation of ECV by use of native and post-contrast T1 maps have been described as the most promising measures of extracellular matrix expansion (11).

Native T1 mapping identifies pathological changes affecting the intracellular or extracellular space, such as myocardial edema in acute myocardial infarction or in myocarditis (17–19), amyloid deposition (20,21), iron overload (22), or glycosphingolipid storage in Anderson-Fabry disease (23). With the use of T1 maps before and after administration of gadolinium-based contrast agents, the ECV can be estimated (8). Elevated ECV as quantified by CMR (CMR-ECV) has been demonstrated in cardiac amyloidosis (24–26), acute myocarditis (27), and hypertrophic cardiomyopathy sarcomere mutation carriers, even in the absence of myocardial hypertrophy (28). Several clinical trials are currently investigating the potential role of T1 mapping in various clinical settings, such as timing of surgery in aortic stenosis (NCT01755936), or are evaluating the cardiotoxic effects of chemotherapy (NCT01719562) (29).

SEE PAGE 24

However, despite a rapidly growing body of evidence indicating the clinical usefulness of this novel technique, its prognostic significance is still not well defined. Furthermore, although inversion recovery methods such as the modified Look-Locker inversion recovery (MOLLI) sequence demonstrate excellent precision and are highly reproducible when tightly controlled protocols are used (30), no final consensus has yet been reached concerning a preferred T1-mapping technique (11). Its reliability is also limited by a lack of validation data against in vivo myocardial biopsies because of heterogeneity of techniques and small patient numbers (**Table 1**) (8,9,13,31–37). Although T1-mapping data appear to have great prognostic potential, only a few studies have reported on the prognostic impact of T1 mapping by CMR (13,38–41).

The present study prospectively evaluates the diagnostic and prognostic significance of CMR T1 mapping for ECV calculation in 473 consecutive patients, of whom 36 underwent left ventricular (LV) biopsy for methodological validation.

ABBREVIATIONS AND ACRONYMS

CABG = coronary artery bypass graft

CMR = cardiac magnetic resonance

ECV = extracellular volume

LGE = late gadolinium enhancement

LV = left ventricular

MOLLI = modified Look-Locker inversion

NT-proBNP = N-terminal prohormone brain natriuretic peptide

RV = right ventricular

METHODS

STUDY DESIGN. This was a prospective, observational study performed at the Medical University of Vienna, approved by the local ethics committee. Between July 2012 and February 2015, 473 consecutive patients without hypertrophic cardiomyopathy, cardiac amyloidosis, or Anderson-Fabry disease referred for CMR were invited to participate. Those patients who also underwent coronary angiography were invited to undergo myocardial biopsy. Written informed consent was collected before study enrollment from all patients. The Medical University of Vienna represents a university-affiliated tertiary care center with a high-volume multimodality-imaging facility.

CLINICAL DEFINITIONS. At the time of CMR, demographic data (age, sex, body mass index, body surface area) and comorbidities were assessed. These included atrial fibrillation (documented episode during the previous 6 months), arterial hypertension (≥140/90 mm Hg or antihypertensive treatment), hypercholesterolemia (total serum cholesterol 240

TABLE 1 Overview of Studies Validating Various T1-Mapping Methods Against Histological Specimens

First Author (Ref. #)	T1-Mapping Method	Patient Population	r and p Values
Flett et al. (8)	EQ-CMR ECV	18 AS and 8 HCM patients	$r^2 = 0.796$, $p < 0.001$
Fontana et al. (33)	ShMOLLI EQ ECV Multiple breath-hold ECV	18 AS patients	$r^2 = 0.685$, $p < 0.001$ $r^2 = 0.589$, $p < 0.001$
White et al. (37)	ShMOLLI single-bolus ECV ShMOLLI EQ ECV	18 AS patients	$r^2 = 0.69$, $p < 0.001$ $r^2 = 0.71$, $p < 0.001$
Bull et al. (32)	ShMOLLI native T1	19 AS patients	$r = 0.655$, $p = 0.002$
Miller et al. (36)	DynEq-CMR MOLLI ECV	6 Explanted hearts	$r^2 = 0.893$, $p = 0.004$
Iles et al. (34)	Multiple breath-hold post contrast	9 Patients with heart failure after orthotopic heart transplantation	$r = -0.70$, $p = 0.003$
Mascherbauer et al. (13)	Multiple breath-hold post contrast	9 Patients with heart failure and preserved ejection fraction	$r = 0.977$, $p < 0.001$
Iles et al. (35)	Multiple breath-hold post contrast	4 Explanted hearts; 8 patients with myectomy for HCM	$r = -0.78$, $p = 0.003$
Aus dem Siepen et al. (31)	MOLLI ECV	24 Patients with DCM	$r = 0.85$, $p < 0.01$

AS = aortic stenosis; CMR = cardiac magnetic resonance; DCM = dilated cardiomyopathy; DynEq = dynamic equilibrium; ECV = extracellular volume; EQ = equilibrium; HCM = hypertrophic cardiomyopathy; (Sh)MOLLI = (shortened) modified Look-Locker inversion recovery sequence.

TABLE 2 Baseline Clinical and CMR Parameters

	All Patients (N = 473)	CMR-ECV <27.0% (n = 237; 50.1%)	CMR-ECV ≥27.0% (n = 236; 49.9%)	p Value
Clinical parameters				
Age, yrs				0.001
Mean ± SD	57.8 ± 17.1	55.3 ± 17.0	60.4 ± 16.9	
Median (IQR)	61.3 (45.9–71.6)	56.8 (43.6–68.9)	65.7 (47.7–73.2)	
Female	49.5	40.9	58.1	<0.001
BMI, kg/m^2				0.037
Mean ± SD	27.5 ± 5.6	27.9 ± 5.2	27.1 ± 5.9	
Median (IQR)	26.9 (23.7–30.6)	27.3 (24.5–30.8)	26.3 (22.9–30.1)	
Hypertension	70.8	62.8	78.3	0.001
Atrial fibrillation	28.3	17.2	38.6	<0.001
Diabetes	17.0	14.9	19.0	0.273
Hyperlipidemia	41.6	43.9	39.5	0.376
Current smoker	22.4	18.8	25.3	0.185
Hospitalized at time of CMR	27.2	27.5	26.9	0.904
CAD	27.4	31.9	23.3	0.056
Previous PCI	10.9	13.4	8.7	0.132
Previous CABG	4.3	5.3	3.4	0.349
Previous MI	10.4	12.8	8.2	0.129
Previous stroke	3.6	3.2	3.9	0.711
eGFR, ml/min/1.73 m^2				0.040
Mean ± SD	78.2 ± 25.4	81.1 ± 24.2	75.5 ± 26.2	
Median (IQR)	76.6 (61.0–94.4)	80.1 (63.8–95.5)	74.4 (55.9–93.4)	
Serum NT-proBNP, pg/ml				<0.001
Mean ± SD	1,847 ± 3,274	583 ± 1,817	1,738 ± 4,110	
Median (IQR)	285 (95–1,050)	160 (45–413)	645 (182–1,761)	
Follow-up, months				0.875
Mean ± SD	13.3 ± 9.0	13.3 ± 9.6	13.3 ± 8.5	
Median (IQR)	12.2 (4.0–21.7)	11.3 (3.8–22.8)	13.1 (4.5–20.5)	
Referral diagnosis				0.002
Heart failure	52.0	43.9	60.2	
VHD	19.9	21.1	18.6	
CAD	11.6	14.8	8.5	
Others	16.5	20.3	12.7	

Continued on the next page

mg/dl or use of cholesterol-lowering medication), diabetes (fasting blood glucose level >126 mg/dl or use of antidiabetic medication), coronary artery disease (coronary artery stenosis >50% or fractional flow reserve <0.8), previous percutaneous coronary intervention, and previous coronary artery bypass grafting (CABG). Previous myocardial infarction was defined by both history and CMR. The estimated glomerular filtration rate was calculated with the simplified Modification of Diet in Renal Disease formula (42).

OUTCOME MEASURES. All patients were prospectively followed up at 6-month intervals by ambulatory visits or telephone calls in case of immobility. The primary endpoint was defined as a composition of hospitalization for cardiovascular reasons (heart failure, acute coronary syndrome, pulmonary embolism, stroke) or cardiac death. Endpoints were adjudicated by our internal adjudication committee (D.B. and C.Z.-T.), blinded to CMR data.

CMR. All patients underwent CMR examinations on a 1.5-T scanner (MAGNETOM Avanto, Siemens Healthcare GmbH, Erlangen, Germany), which consisted of standard protocols that included late gadolinium enhancement (LGE) (0.1 mmol/kg gadobutrol [Gadovist, Bayer Vital GmbH, Leverkusen, Germany]) if the estimated glomerular filtration rate was >30 ml/min/1.73 m^2. Left and right atrial volumes were assessed by the biplane area-length method (43). At the time of insertion of the intravenous cannula, blood was drawn for hematocrit and serum creatinine level measurement. LGE was quantified on short-axis stacks using a semiautomatic approach

TABLE 2 Continued

	All Patients (N = 473)	CMR-ECV <27.0% (n = 237; 50.1%)	CMR-ECV ≥27.0% (n = 236; 49.9%)	p Value
CMR parameters				
LA volume				<0.001
Mean ± SD	111.3 ± 75.0	99.4 ± 73.2	123.5 ± 75.1	
Median (IQR)	93.3 (69.7–133.6)	86.6 (64.3–113.5)	105.7 (76.8–155.2)	
RA volume				0.037
Mean ± SD	95.0 ± 60.8	87.9 ± 55.7	102.3 ± 65.0	
Median (IQR)	81.0 (63.4–106.5)	79.8 (60.3–101.0)	82.8 (65.8–113.9)	
IVS, mm				0.568
Mean ± SD	11.5 ± 2.7	11.5 ± 2.5	11.4 ± 3.0	
Median (IQR)	11.0 (10.0–13.0)	11.0 (10.0–13.0)	11.0 (9.5–13.0)	
LV mass, g				0.092
Mean ± SD	114.4 ± 41.2	119.5 ± 43.5	110.5 ± 39.1	
Median (IQR)	102.5 (86.0–136.5)	113.0 (90.0–144.0)	97.0 (85.0–125.0)	
LVEF				0.511
Mean ± SD	61.5 ± 11.8	62.2 ± 10.6	60.9 ± 12.9	
Median (IQR)	62.0 (56.0–69.0)	63.0 (56.0–69.0)	62.0 (55.0–69.0)	
LVEDVi, ml				0.324
Mean ± SD	77.5 ± 25.0	75.7 ± 22.4	79.3 ± 27.4	
Median (IQR)	71.7 (60.0–88.3)	70.7 (59.8–87.1)	72.5 (60.4–89.6)	
Cardiac index, l/min				0.168
Mean ± SD	3.1 ± 0.9	3.2 ± 0.9	3.1 ± 0.9	
Median (IQR)	3.0 (2.6–3.5)	3.0 (2.6–3.6)	2.9 (2.5–3.4)	
RVEF				0.661
Mean ± SD	56.2 ± 10.1	56.8 ± 9.2	55.5 ± 10.9	
Median (IQR)	57.0 (50.0–63.0)	57.0 (51.0–62.0)	57.0 (49.0–63.0)	
RVEDVi, ml				0.104
Mean ± SD	76.8 ± 21.1	75.0 ± 18.4	78.6 ± 23.4	
Median (IQR)	73.9 (63.3–86.3)	72.6 (62.0–85.4)	76.1 (64.7–86.7)	
Infarct size, % of LV mass*				0.931
Mean ± SD	15.5 ± 6.4	14.8 ± 4.6	16.3 ± 8.0	
Median (IQR)	14.5 (10.8–19.0)	15.0 (12.0–17.0)	14.0 (10.0–19.0)	
CMR-ECV				<0.001
Mean ± SD	27.5 ± 3.9	24.6 ± 1.9	30.4 ± 3.2	
Median (IQR)	27.0 (25.1–29.4)	25.1 (23.6–26.2)	29.4 (28.1–31.6)	

Values are mean ± SD, median (interquartile range), or %. *Among patients with myocardial infarction.

BMI = body mass index; CABG = coronary artery bypass graft surgery; CAD = coronary artery disease; CMR = cardiac magnetic resonance; CMR-ECV = extracellular volume as determined by cardiac magnetic resonance imaging; eGFR = estimated glomerular filtration rate; IQR = interquartile range; IVS = interventricular septal thickness; LA = left atrium; LGE = late gadolinium enhancement; LV = left ventricle; LVEDVi = left ventricular end-diastolic volume indexed to body surface area; LVEF = left ventricular ejection fraction; MI = myocardial infarction; NT-proBNP = N-terminal prohormone brain natriuretic peptide; PCI = percutaneous coronary intervention; RA = right atrium; RVEF = right ventricular ejection fraction; RVEDVi = right ventricular end-diastolic volume indexed to body surface area; VHD = valvular heart disease.

by defining a threshold of 5 SD above mean signal intensity of healthy myocardium (44).

T1 mapping was performed with electrocardiographically triggered MOLLI with a 5(3)3 prototype (5 acquisition heartbeats followed by 3 recovery heartbeats and a further 3 acquisition heartbeats) on a short-axis midcavity slice and with a 4-chamber view. This method generates an inline, pixel-based T1 map by acquiring a series of images over several heartbeats with shifted T1 times, inline motion correction, and inline calculation of the T1 relaxation curve within 1 breath hold. T1-sequence parameters were as follows: starting inversion time (TI) 120 ms, TI increment 80 ms, reconstructed matrix size 256 × 218, measured matrix size 256 × 144 (phase-encoding resolution 66%, phase-encoding field of view 85%). T1 maps were created both before and 15 min after contrast agent application. For post-contrast T1 mapping, a 4(1)3(1)2 prototype was used. Regions of interest were defined as LV myocardium without areas of infarcted myocardium. T1 values (in milliseconds) of the blood pool were derived with sufficient distance to papillary muscles and the endomyocardial border. T1 values from the short-axis and the 4-chamber view were averaged.

FIGURE 1 Cardiac Magnetic Resonance T1 Map and Left Ventricular Histological Specimen

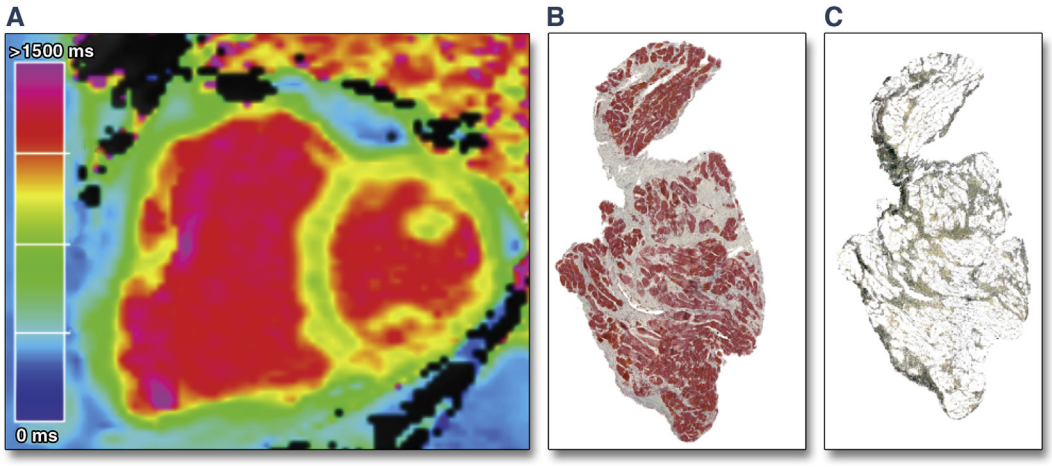

(A) Native T1 map in a patient with heart failure and preserved ejection fraction. Extracellular volume by cardiac magnetic resonance T1 mapping was 26.5%. **(B)** Left ventricular histological specimen of the same patient scanned with TissueFAXS software. **(C)** Same specimen after a color-threshold approach was used to visualize and quantify extracellular matrix (30.7%).

CMR-ECV was calculated with the formula (15)

$$\text{CMR} - \text{ECV} = (1 - \text{hematocrit}) \times \frac{\left(\frac{1}{\text{T1 myo post}}\right) - \left(\frac{1}{\text{T1 myo pre}}\right)}{\left(\frac{1}{\text{T1 blood post}}\right) - \left(\frac{1}{\text{T1 blood pre}}\right)}$$

where T1 myo pre/T1 blood pre indicates myocardial/blood native T1 times and T1 myo post/T1 blood post indicates T1 times of myocardium/blood 15 min after contrast agent application. Figure 1A shows a T1 map of a heart failure patient.

For further CMR analyses dedicated software (cmr42, Circle Cardiovascular Imaging Inc., Calgary, Alberta, Canada) was used.

MYOCARDIAL BIOPSY AND HISTOLOGICAL ANALYSIS. Biopsy samples were taken from the LV free wall during left-sided heart catheterization by use of dedicated devices (Bipal biopsy forceps, Cordis Corporation, Bridgewater, New Jersey). Specimens were embedded in paraffin, stained with modified trichrome as described previously (45), and scanned at 20-fold magnification with a high-resolution microscope and TissueFAXS software (TissueGnostics, Vienna, Austria). ECV determined by this method (TissueFAXS-ECV) was quantified with ImageJ software (46) with a color-threshold macro based on an algorithm by G. Landini (version 1.12) (47). Endocardium, blood vessels, and perivascular tissue were excluded from the analysis. Figure 1B shows a histological specimen of a patient with heart failure; Figure 1C displays TissueFAXS-ECV in the same specimen after the exclusion of cardiomyocytes.

STATISTICAL ANALYSIS. Continuous data are expressed as mean ± SD or as median with corresponding interquartile range, and categorical variables are presented as percentages or total numbers. Differences between 2 groups were analyzed with the Wilcoxon rank sum test. Chi-square tests or Fisher exact tests were used for categorical variables as appropriate.

FIGURE 2 Patient Population

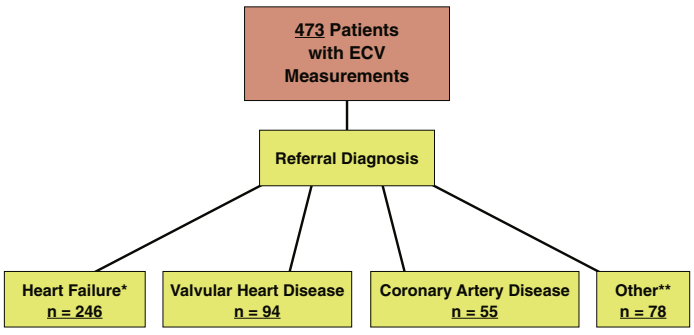

A total of 473 patients underwent cardiac magnetic resonance imaging that included assessment of extracellular volume (ECV). Referral diagnoses are displayed. *Included patients with preserved and reduced ejection fraction. **Sarcoidosis (n = 45), Duchenne muscular dystrophy gene carriers (n = 21), pericardial effusion (n = 6), cardiac tumors (n = 4), and aortic aneurysm (n = 2).

Survival analyses were performed by Kaplan-Meier estimates and Cox regression analysis. All parameters with a significant influence in the univariable model entered the multiple regression analysis by use of a stepwise selection. The multivariable model was run for clinical and imaging parameters separately. Clinical and imaging parameters independently associated with outcome were entered into an additional combined multivariable model.

Pearson correlation coefficients were used to report the relationship between CMR and histological findings. By Bland-Altman plots, agreement between CMR-ECV and TissueFAXS-ECV was visualized and reported as mean difference and corresponding 95% confidence interval (±1.96 SD). For all tests, the significance level was set to $p \leq 0.05$.

RESULTS

BASELINE CHARACTERISTIC AND CMR PARAMETERS. A total of 473 patients (49.5% female, age 57.8 ± 17.1 years) were included. Table 2 lists patient baseline characteristics and imaging parameters stratified according to median CMR-ECV (27.0%). Patients with higher ECV were more often female ($p < 0.001$), older ($p = 0.001$), more frequently hypertensive ($p = 0.001$), and in atrial fibrillation ($p < 0.001$). Furthermore, they had worse renal function ($p = 0.040$) and higher serum levels of N-terminal prohormone brain natriuretic peptide (NT-proBNP; $p < 0.001$) and presented with larger left and right atrial volumes ($p < 0.001$ and $p = 0.037$, respectively). Referral diagnoses are shown in Figure 2.

CORRELATION BETWEEN ECV BY HISTOLOGY AND CMR. Thirty-six patients underwent LV biopsy. Of these, 28 had heart failure and 8 had valvular heart disease. No LGE was present in the LV free wall where biopsy samples were taken.

TissueFAXS-ECV was 26.3 ± 7.2% on average. CMR-ECV was significantly correlated with histological ECV (Figure 3) ($r = 0.493$, $p = 0.002$). Bland-Altman analysis (Figure 4) revealed acceptable agreement between CMR-ECV and TissueFAXS-ECV, with a mean difference of −2.3% (limits of agreement: −14.7% and 10.0%) between CMR-ECV and TissueFAXS-ECV. There was a proportional bias because of a higher variability of TissueFAXS-ECV (interquartile range: 13.7% to 38.7%; 26.3 ± 7.2%) than CMR-ECV (interquartile range: 23.6% to 35.5%; 28.6 ± 2.9%). Therefore, CMR-ECV measurements tended to exceed the TissueFAXS-ECV measurements for low average values, whereas the opposite was the case for high average values.

FIGURE 3 Correlation Between ECV by Cardiac Magnetic Resonance T1 Mapping and TissueFAXS Analysis

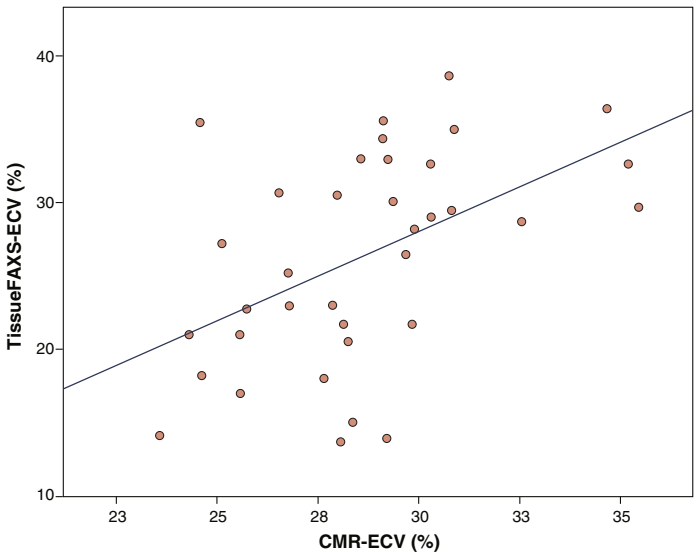

Correlation between extracellular volume (ECV) by cardiac magnetic resonance T1 mapping (CMR-ECV) and by TissueFAXS (Tissue-FAXS ECV) in 36 left ventricular specimens ($r = 0.493$, $p = 0.002$).

FIGURE 4 Bland-Altman Plot Demonstrating Good Agreement of TissueFAXS-ECV and CMR-ECV

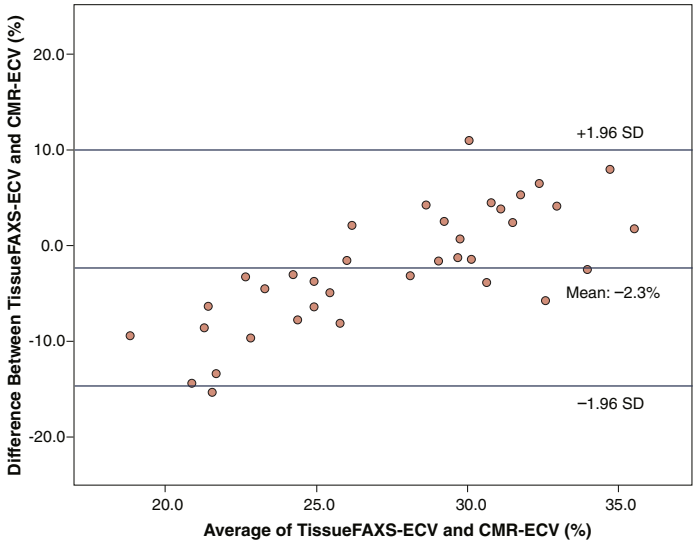

Mean difference was −2.3% (limits of agreement: −14.7% and 10.0%). CMR-ECV = extracellular volume as determined by cardiac magnetic resonance imaging T1 mapping; TissueFAXS-ECV = extracellular volume as determined by TissueFAXS.

FIGURE 5 Kaplan-Meier Plot for Event-Free Survival, Stratified by Tertiles of CMR-ECV

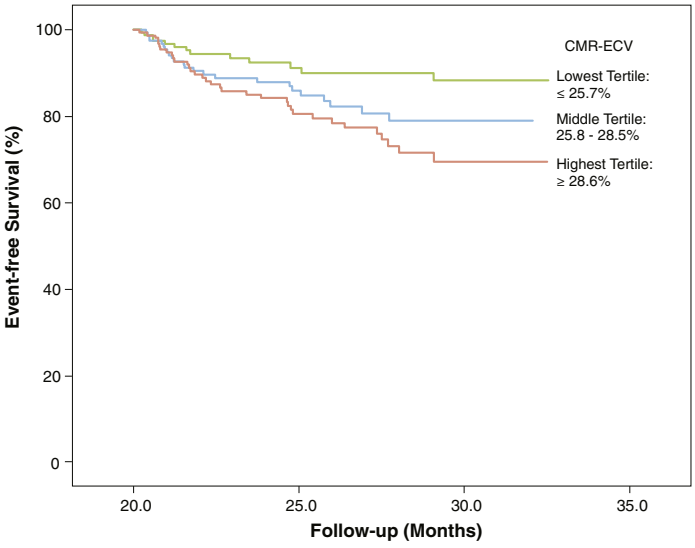

Log-rank test, p = 0.013. CMR-ECV = extracellular volume as determined by cardiac magnetic resonance imaging T1 mapping.

OUTCOME ANALYSIS. Patients were followed up for 13.3 ± 9.0 months. Follow-up was complete in all patients. In total, 71 patients (15.0%) experienced a cardiac event (60 hospitalizations for cardiovascular reasons, 11 cardiac deaths). The following parameters were significantly different between patients with and without cardiac events (Online Table 1): patients with events were older ($p < 0.001$); more frequently had arterial hypertension ($p < 0.001$), atrial fibrillation ($p < 0.001$), diabetes ($p = 0.016$), and hyperlipidemia ($p = 0.036$); and were more often hospitalized at the time of CMR ($p = 0.004$). They furthermore presented with more frequent coronary artery disease ($p = 0.027$), previous CABG ($p = 0.001$), previous myocardial infarction ($p = 0.047$), worse renal function ($p = 0.001$), higher serum NT-proBNP levels ($p < 0.001$), a thicker interventricular septum ($p = 0.006$), and more dilated left and right atria ($p = 0.007$ and $p = 0.001$, respectively). Cardiac index was worse among patients with cardiac events ($p = 0.010$), and CMR-ECV was significantly higher ($p < 0.001$).

By Kaplan-Meier analysis (Figure 5), higher CMR-ECV was associated with an increased event rate (log-rank test $p = 0.013$). Table 3 displays results of the univariable and multivariable Cox regression analysis. Among clinical parameters with significant influence in the univariable model, age ($p = 0.008$), atrial fibrillation ($p = 0.004$), and previous CABG ($p = 0.048$) were independently associated with outcome. Among imaging variables, right ventricular (RV) size ($p = 0.007$), and CMR-ECV ($p = 0.004$) remained significantly related to event-free survival in the multivariable Cox regression analysis. When clinical and imaging parameters were included in a combined model, only age ($p = 0.001$), atrial fibrillation ($p = 0.035$), previous CABG ($p = 0.033$), and RV size ($p = 0.004$) were independently associated with outcome (Table 4).

DISCUSSION

The present study evaluated the diagnostic accuracy and prognostic value of CMR-ECV. We have demonstrated that ECV calculation by CMR T1 mapping accurately reflects the actual amount of extracellular matrix expansion by histology and provided evidence for the prognostic and diagnostic usefulness of this novel technique in a large and well-characterized patient cohort.

CMR T1 mapping has recently awakened great hope because it allows quantitative myocardial tissue characterization (11,14,15,20,22,34,48). It has been advertised as an important diagnostic tool in patients with cardiac amyloidosis, in which high native T1 times and ECV by CMR are found (21,25), as well as in Anderson-Fabry disease, which is characterized by low myocardial native T1 times (23). In addition, for acute myocarditis, promising results have been published, indicating more precise detection of the disease by T1 mapping than by conventional CMR (49,50).

HISTOLOGICAL VALIDATION OF T1-MAPPING TECHNIQUES. Considerable efforts have been undertaken to validate T1 mapping (8,9,13,31-37). Table 1 summarizes previous studies that reported validation data of CMR T1 mapping against myocardial biopsy samples. Various T1-mapping techniques have been applied, including equilibrium contrast T1 mapping (8,33,36,37), shortened MOLLI single bolus (37), shortened MOLLI native T1 (32), and multiple breath-hold post-contrast T1 mapping (13,34,35). Most of these studies included small patient numbers. The various T1-mapping techniques further limit their comparability; however, all studies indicate that the amount of ECV detected by T1 maps reflects actual extracellular matrix expansion and/or disease severity. The present investigation adds substantially to the existing evidence because it provides validation data from 36 patients who underwent in vivo LV biopsy. Our data show good correlation and agreement between ECV as calculated by CMR T1 mapping and ECV by TissueFAXS from histology (Figures 3 and 4).

ECV BY T1 MAPPING: A RELIABLE PROGNOSTIC MARKER? So far, little is known about the prognostic

value of ECV by CMR T1 mapping, a question that has only been addressed in a few published series. We previously showed that extracellular matrix expansion, reflected by shorter multiple breath-hold post-contrast T1 times, was associated with an increased adverse event rate in patients with heart failure with preserved ejection fraction (13). Wong et al. (38) investigated 793 patients without cardiac amyloidosis or hypertrophic cardiomyopathy; they reported a significant impact of ECV by CMR T1 mapping on outcome after adjusting for age, LV ejection fraction, and infarction size. Ghosn et al. (39) recently presented preliminary data on an independent association between CMR-ECV and event-free survival in 1,247 patients. Neilan et al. (40) studied 145 patients with recurrent atrial fibrillation undergoing pulmonary vein isolation and found that CMR-ECV was associated with worse outcome.

The present study evaluates the prognostic value of CMR-ECV in 473 consecutive patients after correction for a large number of cardiovascular comorbidities, listed in Table 3. Importantly, NT-proBNP serum level, renal function, atrial fibrillation, and previous heart surgery, as well as imaging parameters such as left and right atrial and RV size, which have not been analyzed previously in the context of CMR T1 mapping, were included. Among imaging variables, CMR-ECV and RV size were independently associated with outcome. However, when clinical variables were included in the Cox model, only age, atrial fibrillation, previous CABG, and RV size but not CMR-ECV remained significantly associated with event-free survival. To clarify whether differences between our results and the findings by Wong et al. (38) may be due to the inclusion of more clinical variables, we restricted a second analysis to only those variables that were assessed by Wong et al. (38) (age, CMR-ECV, LV ejection fraction, and infarct size). In that analysis, CMR-ECV was also independently associated with survival among clinical variables in our cohort. Thus, discrepancies between previous studies (38,39) and our results appear to arise from the inclusion of additional clinical parameters.

FUTURE OUTLOOK. T1 mapping certainly has the potential to provide insights into pathogenic processes, to detect diseases at a very early stage, non-invasively monitor disease progress, or even guide therapy. New applications of T1 mapping currently being investigated include monitoring the cardiotoxic effects of chemotherapy (NCT01719562) and cardiac involvement in human immunodeficiency virus-positive individuals (NCT02054494) (29). Further work over long follow-up periods will be needed to increase our knowledge about the prognostic impact of T1 mapping in various diseases.

TABLE 3 Univariable and Multivariable Cox Regression Analysis With Stepwise Selection

	Univariable		Multivariable	
	p Value	HR (95% CI)	p Value	HR (95% CI)
Clinical parameters				
Age	<0.001	1.054 (1.035–1.073)	0.008	1.030 (1.008–1.053)
Female	0.877	1.038 (0.651–1.654)		
BMI	0.070	1.034 (0.997–1.073)		
Hypertension	0.001	3.685 (1.765–7.692)		
Atrial fibrillation	<0.001	3.587 (2.237–5.752)	0.004	2.208 (1.282–3.803)
Diabetes	0.043	1.723 (1.018–2.916)		
Hyperlipidemia	0.092	1.497 (0.936–2.395)		
Current smoker	0.639	1.150 (0.641–2.065)		
Hospitalized at time of CMR	0.023	1.732 (1.079–2.781)		
CAD	0.057	1.593 (0.986–2.573)		
Previous PCI	0.104	1.674 (0.899–3.117)		
Previous CABG	0.003	3.013 (1.442–6.294)	0.048	2.228 (1.008–4.924)
Previous MI	0.111	1.657 (0.890–3.083)		
Previous stroke	0.410	1.529 (0.557–4.194)		
eGFR	<0.001	0.981 (0.971–0.991)		
Serum NT-proBNP*	<0.001	1.812 (1.431–2.294)		
Imaging parameters				
LA volume	0.011	1.003 (1.001–1.005)		
RA volume	<0.001	1.005 (1.002–1.007)		
IVS	0.029	1.186 (1.008–1.169)		
LV mass	0.388	0.995 (0.985–1.006)		
LVEF	0.710	1.004 (0.983–1.026)		
LVEDVi	0.930	1.000 (0.990–1.009)		
Cardiac index	0.056	0.749 (0.557–1.007)		
RVEF	0.163	0.983 (0.960–1.007)		
RVEDVi	0.001	1.015 (1.006–1.023)	0.007	1.012 (1.003–1.021)
Infarction size†	0.539	0.958 (0.837–1.098)		
CMR-ECV	<0.001	1.108 (1.053–1.165)	0.004	1.092 (1.028–1.160)

Analyses were run for clinical and imaging variables separately. *NT-proBNP was graded into quartiles for this analysis. †Per 1% increase among patients with previous MI.

CI = confidence interval; HR = hazard ratio; other abbreviations as in Table 2.

STUDY LIMITATIONS. The data presented have been collected in a single-center setting. Therefore, a center-specific bias cannot be excluded. However, the major advantages of limiting data collection to a

TABLE 4 Multivariable Cox Regression Analysis Including Clinical and Imaging Variables That Were Significant Within the Respective Group in the Multivariable Analysis (Table 3) in a Model Using Forced Entry

			Combined: Multivariable	
	p Value	HR (95% CI)	p Value	HR (95% CI)
Clinical: Multivariable				
Age	0.008	1.030 (1.030–1.053)	0.001	1.033 (1.013–1.054)
Atrial fibrillation	0.004	2.208 (1.282–3.803)	0.035	1.815 (1.042–3.164)
Previous CABG	0.048	2.228 (1.008–4.924)	0.033	2.261 (1.067–4.788)
Imaging: Multivariable				
RVEDVi	0.007	1.012 (1.003–1.021)	0.004	1.011 (1.004–1.019)
CMR-ECV	0.004	1.092 (1.028–1.160)	0.497	1.022 (0.960–1.087)

Abbreviations as in Table 2.

single center are (1) adherence to a constant clinical routine, (2) constant quality of work-up, and (3) constant follow-up.

With regard to myocardial biopsy, it has to be noted that during left-sided heart catheterization, only small myocardial specimens can be retrieved. The distribution and extent of extracellular matrix in such specimens does not necessarily reflect extracellular matrix expansion across the entire LV myocardium. However, we found a significant correlation between ECV on CMR T1 mapping and histological ECV.

The majority of our patients (85%) presented with normal or preserved LV systolic function (LV ejection fraction >50%). Our results may therefore not be transferable to other patient populations with reduced LV function.

Studies based on T1-mapping results are furthermore limited by the lack of a standardized T1-mapping approach. In the present study, we used one of the standard T1-mapping sequences (see the Methods section).

CONCLUSIONS

CMR T1 mapping is a promising technique that allows accurate estimation of the extent of myocardial extracellular matrix expansion compared with biopsies. Among imaging parameters, CMR-ECV has great prognostic potential; however, its additive value in conjunction with established clinical factors has yet to be defined.

REPRINT REQUESTS AND CORRESPONDENCE: Dr. Julia Mascherbauer, Division of Cardiology, Medical University of Vienna, Waehringer Guertel 18-20, 1090 Vienna, Austria. E-mail: julia.mascherbauer@meduniwien.ac.at.

PERSPECTIVES

COMPETENCY IN MEDICAL KNOWLEDGE: T1 mapping by CMR allows accurate noninvasive estimation of ECV when compared with myocardial biopsies. Among imaging parameters, T1 mapping has great prognostic potential; however, its additive value on top of established clinical factors has yet to be defined.

TRANSLATIONAL OUTLOOK: T1 mapping has the potential to provide insights into pathogenic processes, detect diseases at a very early stage, noninvasively monitor disease progress, or even guide therapy.

REFERENCES

1. Conrad CH, Brooks WW, Hayes JA, Sen S, Robinson KG, Bing OH. Myocardial fibrosis and stiffness with hypertrophy and heart failure in the spontaneously hypertensive rat. Circulation 1995;91:161–70.

2. Kass DA, Bronzwaer JG, Paulus WJ. What mechanisms underlie diastolic dysfunction in heart failure? Circ Res 2004;94:1533–42.

3. Mann DL. Mechanisms and models in heart failure: a combinatorial approach. Circulation 1999;100:999–1008.

4. Mohammed SF, Hussain S, Mirzoyev SA, Edwards WD, Maleszewski JJ, Redfield MM. Coronary microvascular rarefaction and myocardial fibrosis in heart failure with preserved ejection fraction. Circulation 2015;131:550–9.

5. Heling A, Zimmermann R, Kostin S, et al. Increased expression of cytoskeletal, linkage, and extracellular proteins in failing human myocardium [published correction appears in Circ Res 2000;87:167]. Circ Res 2000;86:846–53.

6. Maisch B. Ventricular remodeling. Cardiology 1996;87 Suppl 1:2–10.

7. Sun Y, Weber KT. Cardiac remodelling by fibrous tissue: role of local factors and circulating hormones. Ann Med 1998;30 Suppl 1:3–8.

8. Flett AS, Hayward MP, Ashworth MT, et al. Equilibrium contrast cardiovascular magnetic resonance for the measurement of diffuse myocardial fibrosis: preliminary validation in humans. Circulation 2010;122:138–44.

9. Messroghli DR, Nordmeyer S, Dietrich T, et al. Assessment of diffuse myocardial fibrosis in rats using small-animal Look-Locker inversion recovery T1 mapping. Circ Cardiovasc Imaging 2011;4:636–40.

10. Messroghli DR, Plein S, Higgins DM, et al. Human myocardium: single-breath-hold MR T1 mapping with high spatial resolution–reproducibility study. Radiology 2006;238:1004–12.

11. Moon JC, Messroghli DR, Kellman P, et al. Myocardial T1 mapping and extracellular volume quantification: a Society for Cardiovascular Magnetic Resonance (SCMR) and CMR Working Group of the European Society of Cardiology consensus statement. J Cardiovasc Magn Reson 2013;15:92.

12. Rogers T, Dabir D, Mahmoud I, et al. Standardization of T1 measurements with MOLLI in differentiation between health and disease: the ConSept study. J Cardiovasc Magn Reson 2013;15:78.

13. Mascherbauer J, Marzluf BA, Tufaro C, et al. Cardiac magnetic resonance postcontrast T1 time is associated with outcome in patients with heart failure and preserved ejection fraction. Circ Cardiovasc Imaging 2013;6:1056–65.

14. Kellman P, Wilson JR, Xue H, et al. Extracellular volume fraction mapping in the myocardium, part 2: initial clinical experience. J Cardiovasc Magn Reson 2012;14:64.

15. Kellman P, Wilson JR, Xue H, Ugander M, Arai AE. Extracellular volume fraction mapping in the myocardium, part 1: evaluation of an automated method. J Cardiovasc Magn Reson 2012;14:63.

16. Fernandes JL, Rochitte CE. T1 mapping: technique and applications. Magn Reson Imaging Clin N Am 2015;23:25–34.

17. Messroghli DR, Niendorf T, Schulz-Menger J, Dietz R, Friedrich MG. T1 mapping in patients with acute myocardial infarction. J Cardiovasc Magn Reson 2003;5:353–9.

18. Ugander M, Bagi PS, Oki AJ, et al. Myocardial edema as detected by pre-contrast T1 and T2 CMR delineates area at risk associated with acute myocardial infarction. J Am Coll Cardiol Img 2012;5:596–603.

19. Ferreira VM, Piechnik SK, Dall'Armellina E, et al. Non-contrast T1-mapping detects acute myocardial edema with high diagnostic accuracy: a comparison to T2-weighted cardiovascular magnetic resonance. J Cardiovasc Magn Reson 2012;14:42.

20. Karamitsos TD, Piechnik SK, Banypersad SM, et al. Noncontrast T1 mapping for the diagnosis of cardiac amyloidosis. J Am Coll Cardiol Img 2013;6:488–97.

21. Fontana M, Banypersad SM, Treibel TA, et al. Native T1 mapping in transthyretin amyloidosis. J Am Coll Cardiol Img 2014;7:157–65.

22. Sado DM, White JA, Piechnik SK, et al. Native T1 lowering in iron overload and Anderson Fabry disease: a novel and early marker of disease. J Cardiovasc Magn Reson 2013;15 Suppl 1:O71.

23. Sado DM, White SK, Piechnik SK, et al. Identification and assessment of Anderson-Fabry disease by cardiovascular magnetic resonance noncontrast myocardial T1 mapping. Circ Cardiovasc Imaging 2013;6:392–8.

24. Bandula S, Banypersad SM, Sado D, et al. Measurement of tissue interstitial volume in healthy patients and those with amyloidosis with equilibrium contrast-enhanced MR imaging. Radiology 2013;268:858–64.

25. Banypersad SM, Sado DM, Flett AS, et al. Quantification of myocardial extracellular volume fraction in systemic AL amyloidosis: an equilibrium contrast cardiovascular magnetic resonance study. Circ Cardiovasc Imaging 2013;6:34–9.

26. Mongeon FP, Jerosch-Herold M, Coelho-Filho OR, Blankstein R, Falk RH, Kwong RY. Quantification of extracellular matrix expansion by CMR in infiltrative heart disease. J Am Coll Cardiol Img 2012;5:897–907.

27. Radunski UK, Lund GK, Stehning C, et al. CMR in patients with severe myocarditis: diagnostic value of quantitative tissue markers including extracellular volume imaging. J Am Coll Cardiol Img 2014;7:667–75.

28. Ho CY, Abbasi SA, Neilan TG, et al. T1 measurements identify extracellular volume expansion in hypertrophic cardiomyopathy sarcomere mutation carriers with and without left ventricular hypertrophy. Circ Cardiovasc Imaging 2013;6:415–22.

29. Bulluck H, Maestrini V, Rosmini S, et al. Myocardial T1 mapping. Circ J 2015;79:487–94.

30. Kellman P, Hansen MS. T1-mapping in the heart: accuracy and precision. J Cardiovasc Magn Reson 2014;16:2.

31. Aus dem Siepen F, Buss SJ, Messroghli D, et al. T1 mapping in dilated cardiomyopathy with cardiac magnetic resonance: quantification of diffuse myocardial fibrosis and comparison with endomyocardial biopsy. Eur Heart J Cardiovasc Imaging 2014;16:210–6.s.

32. Bull S, White SK, Piechnik SK, et al. Human non-contrast T1 values and correlation with histology in diffuse fibrosis. Heart 2013;99:932–7.

33. Fontana M, White SK, Banypersad SM, et al. Comparison of T1 mapping techniques for ECV quantification: histological validation and reproducibility of ShMOLLI versus multibreath-hold T1 quantification equilibrium contrast CMR. J Cardiovasc Magn Reson 2012;14:88.

34. Iles L, Pfluger H, Phrommintikul A, et al. Evaluation of diffuse myocardial fibrosis in heart failure with cardiac magnetic resonance contrast-enhanced T1 mapping. J Am Coll Cardiol 2008;52:1574–80.

35. Iles LM, Ellims AH, Llewellyn H, et al. Histological validation of cardiac magnetic resonance analysis of regional and diffuse interstitial myocardial fibrosis. Eur Heart J Cardiovasc Imaging 2015;16:14–22.

36. Miller CA, Naish JH, Bishop P, et al. Comprehensive validation of cardiovascular magnetic resonance techniques for the assessment of myocardial extracellular volume. Circ Cardiovasc Imaging 2013;6:373–83.

37. White SK, Sado DM, Fontana M, et al. T1 mapping for myocardial extracellular volume measurement by CMR: bolus only versus primed infusion technique. J Am Coll Cardiol Img 2013;6:955–62.

38. Wong TC, Piehler K, Meier CG, et al. Association between extracellular matrix expansion quantified by cardiovascular magnetic resonance and short-term mortality. Circulation 2012;126:1206–16.

39. Ghosn MG, Pickett S, Brunner G, et al. Association of myocardial extracellular volume and clinical outcome: a cardiac magnetic resonance study. J Am Coll Cardiol 2015;65:A1077.

40. Neilan TG, Mongeon FP, Shah RV, et al. Myocardial extracellular volume expansion and the risk of recurrent atrial fibrillation after pulmonary vein isolation. JACC Cardiovascular imaging 2014;7:1–11.

41. Banypersad SM, Fontana M, Maestrini V, et al. T1 mapping and survival in systemic light-chain amyloidosis. Eur Heart J 2015;36:244–51.

42. Levey AS, Coresh J, Greene T, et al. Expressing the Modification of Diet in Renal Disease Study equation for estimating glomerular filtration rate with standardized serum creatinine values. Clin Chem 2007;53:766–72.

43. Sievers B, Kirchberg S, Addo M, Bakan A, Brandts B, Trappe HJ. Assessment of left atrial volumes in sinus rhythm and atrial fibrillation using the biplane area-length method and cardiovascular magnetic resonance imaging with TrueFISP. J Cardiovasc Magn Reson 2004;6:855–63.

44. Bondarenko O, Beek AM, Hofman MB, et al. Standardizing the definition of hyperenhancement in the quantitative assessment of infarct size and myocardial viability using delayed contrast-enhanced CMR. J Cardiovasc Magn Reson 2005;7:481–5.

45. Garvey W, Fathi A, Bigelow F, Carpenter B, Jimenez C. A combined elastic, fibrin and collagen stain. Stain Technol 1987;62:365–8.

46. Rasband WS. ImageJ, U.S. National Institutes of Health, Bethesda, Maryland, USA. Available at: http://imagej.nih.gov/ij/. Accessed 19, July, 2015.

47. G. Landini Software. Available at: http://www.mecourse.com/landinig/software/software.html. Accessed November 19, 2015.

48. Ugander M, Oki AJ, Hsu LY, et al. Extracellular volume imaging by magnetic resonance imaging provides insights into overt and sub-clinical myocardial pathology. Eur Heart J 2012;33:1268–78.

49. Ferreira VM, Piechnik SK, Dall'Armellina E, et al. Native T1-mapping detects the location, extent and patterns of acute myocarditis without the need for gadolinium contrast agents. J Cardiovasc Magn Reson 2014;16:36.

50. Dall'Armellina E, Ferreira VM, Kharbanda RK, et al. Diagnostic value of pre-contrast T1 mapping in acute and chronic myocardial infarction. J Am Coll Cardiol Img 2013;6:739–42.

KEY WORDS cardiac magnetic resonance imaging, extracellular matrix, outcome, T1 mapping

APPENDIX For an expanded results section, please see the online version of this article.